Saliency Detection via Cellular Automata
Supplementary Materials

Yao Qin, Huchuan Lu, Yiqun Xu and He Wang
Dalian University of Technology

We compare more saliency maps generated by our proposed algorithm BSCA and MCA with state-of-the-art methods, including IT98 [5], FT09 [1], CA10 [4], RC11 [3], XL13 [10], LR12 [9], HS13 [11], UFO13 [6], RB14 [12]. We display the results tested on five public datasets: ASD [1], MSRA-5000 [8], THUS [2], ECSSD [11] and PASCAL-S [7].

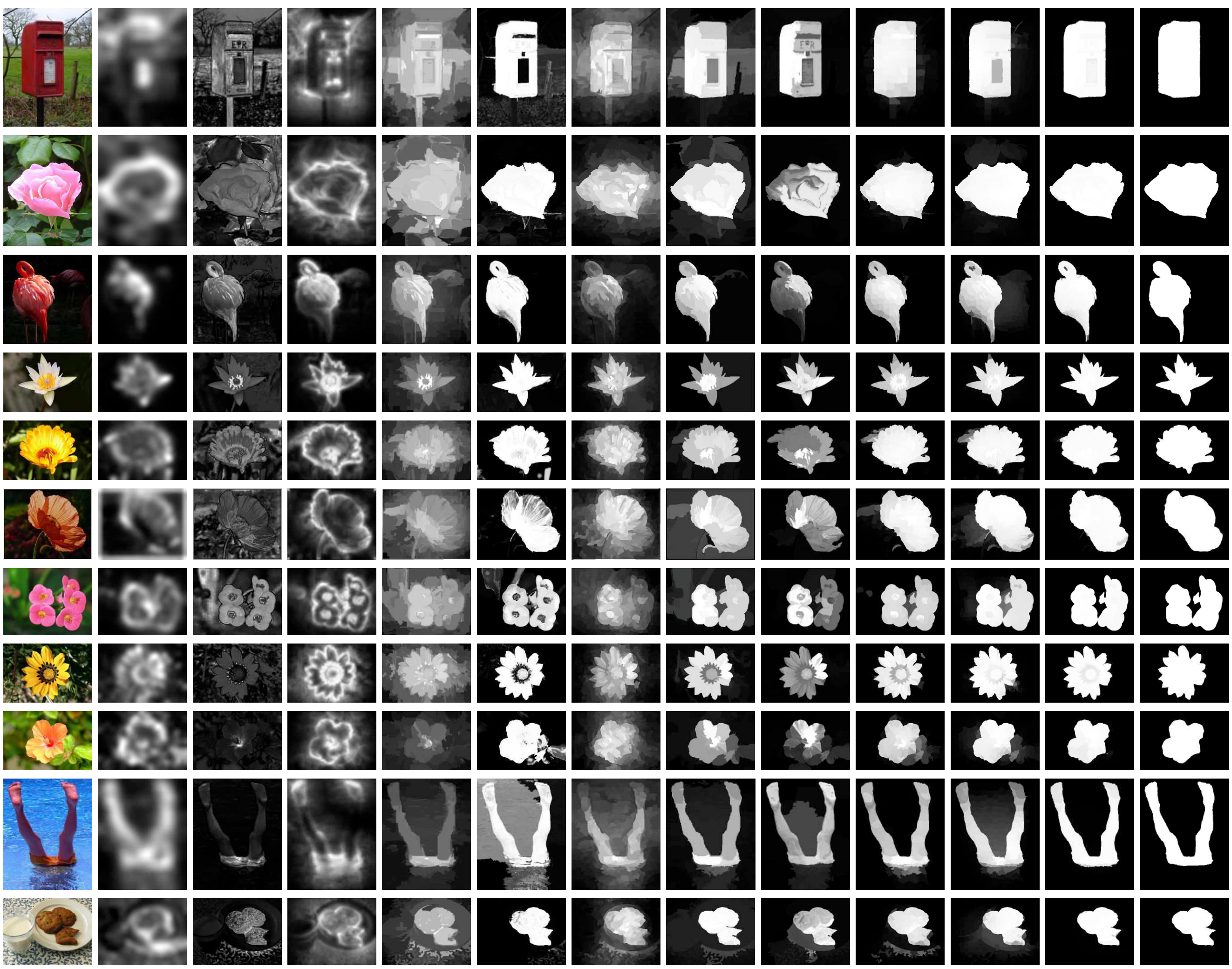

(a) Input (b) IT (c) FT (d) CA (e) RC (f) XL (g) LR (h) HS (i) UFO (j) RB (k) BSCA (l) MCA (m) GT

Figure 1. Comparison of different saliency maps on ASD. BSCA: The background-based maps optimized by Single-layer Cellular Automata. MCA: The integrated saliency maps via Multi-layer Cellular Automata. GT: Ground Truth.

978-1-4673-6964-0/15/$31.00 ©2015 IEEE

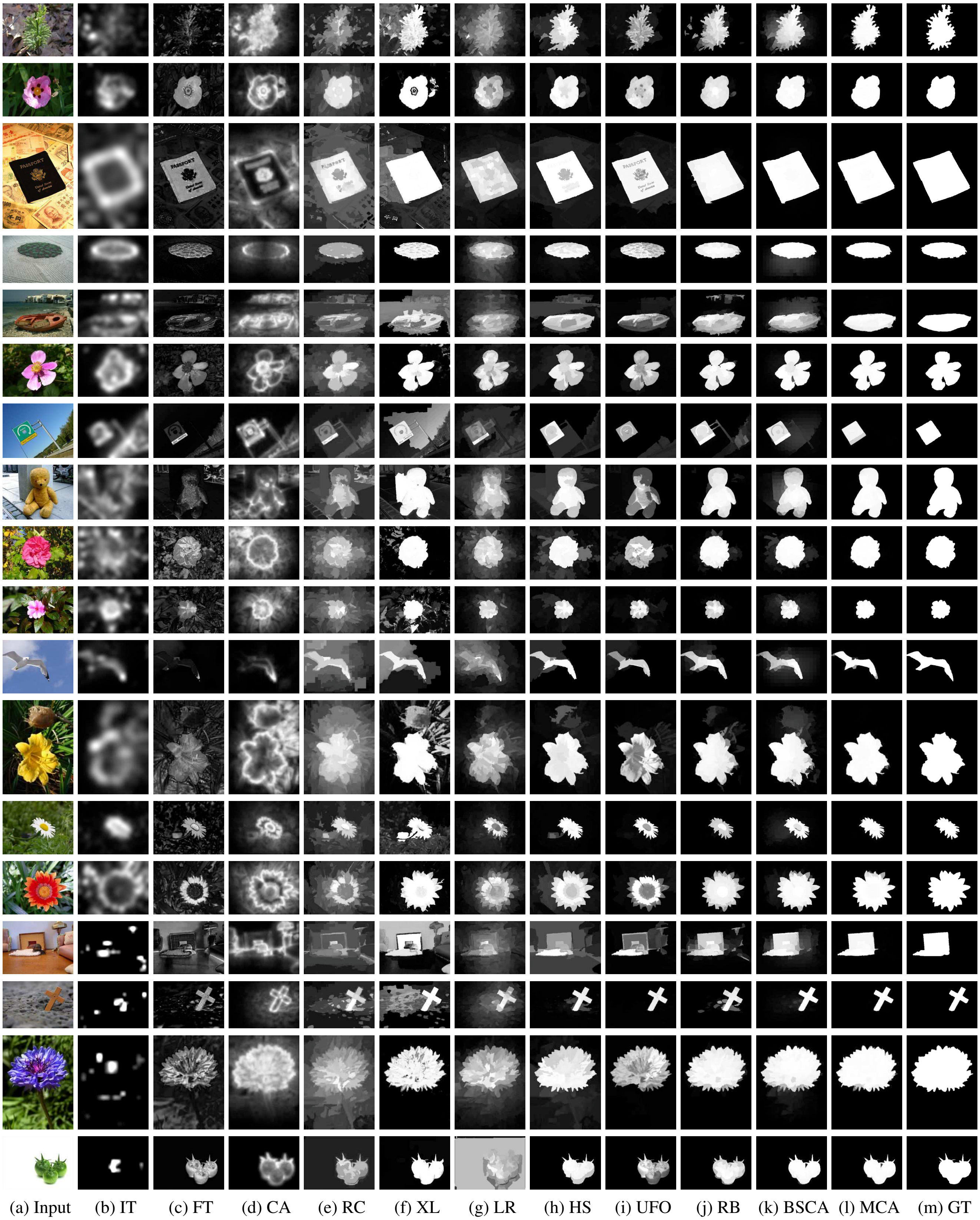

Figure 2. Comparison of different saliency maps on MSRA-5000. BSCA: The background-based maps optimized by Single-layer Cellular Automata. MCA: The integrated saliency maps via Multi-layer Cellular Automata. GT: Ground Truth.

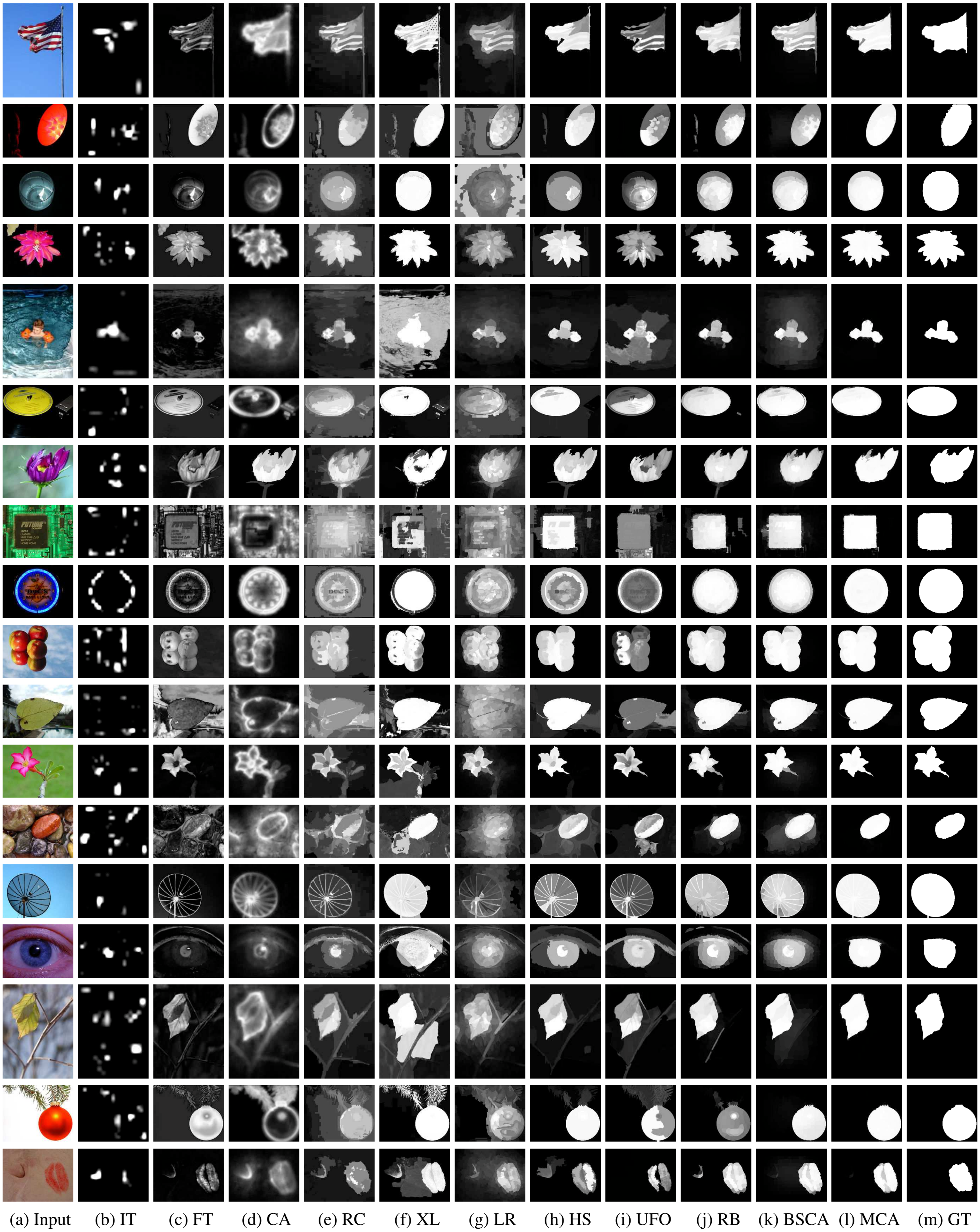

Figure 3. Comparison of different saliency maps on THUS-10000. BSCA: The background-based maps optimized by Single-layer Cellular Automata. MCA: The integrated saliency maps via Multi-layer Cellular Automata. GT: Ground Truth.

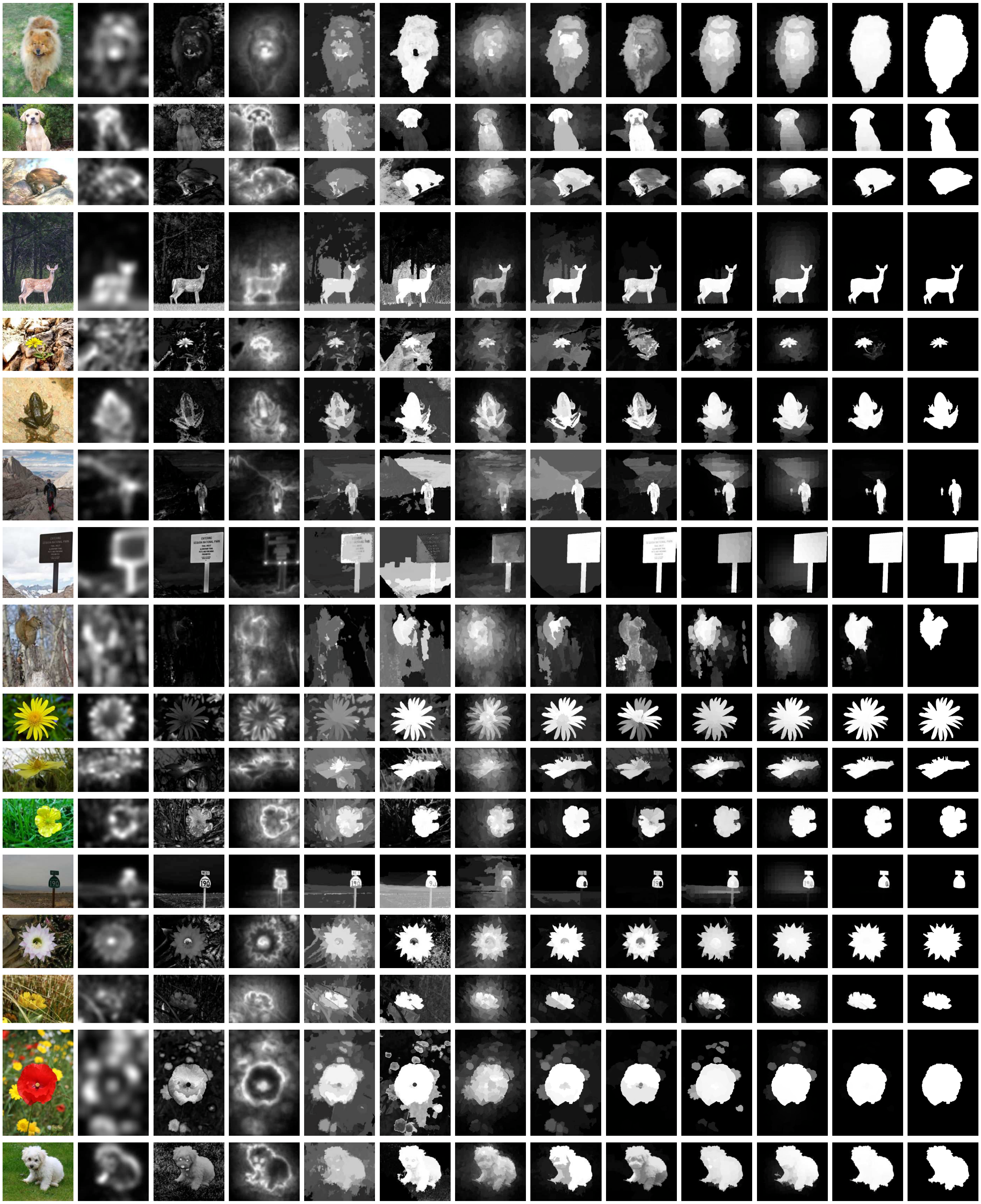

(a) Input (b) IT (c) FT (d) CA (e) RC (f) XL (g) LR (h) HS (i) UFO (j) RB (k) BSCA (l) MCA (m) GT

Figure 4. Comparison of different saliency maps on ECSSD. BSCA: The background-based maps optimized by Single-layer Cellular Automata. MCA: The integrated saliency maps via Multi-layer Cellular Automata. GT: Ground Truth.

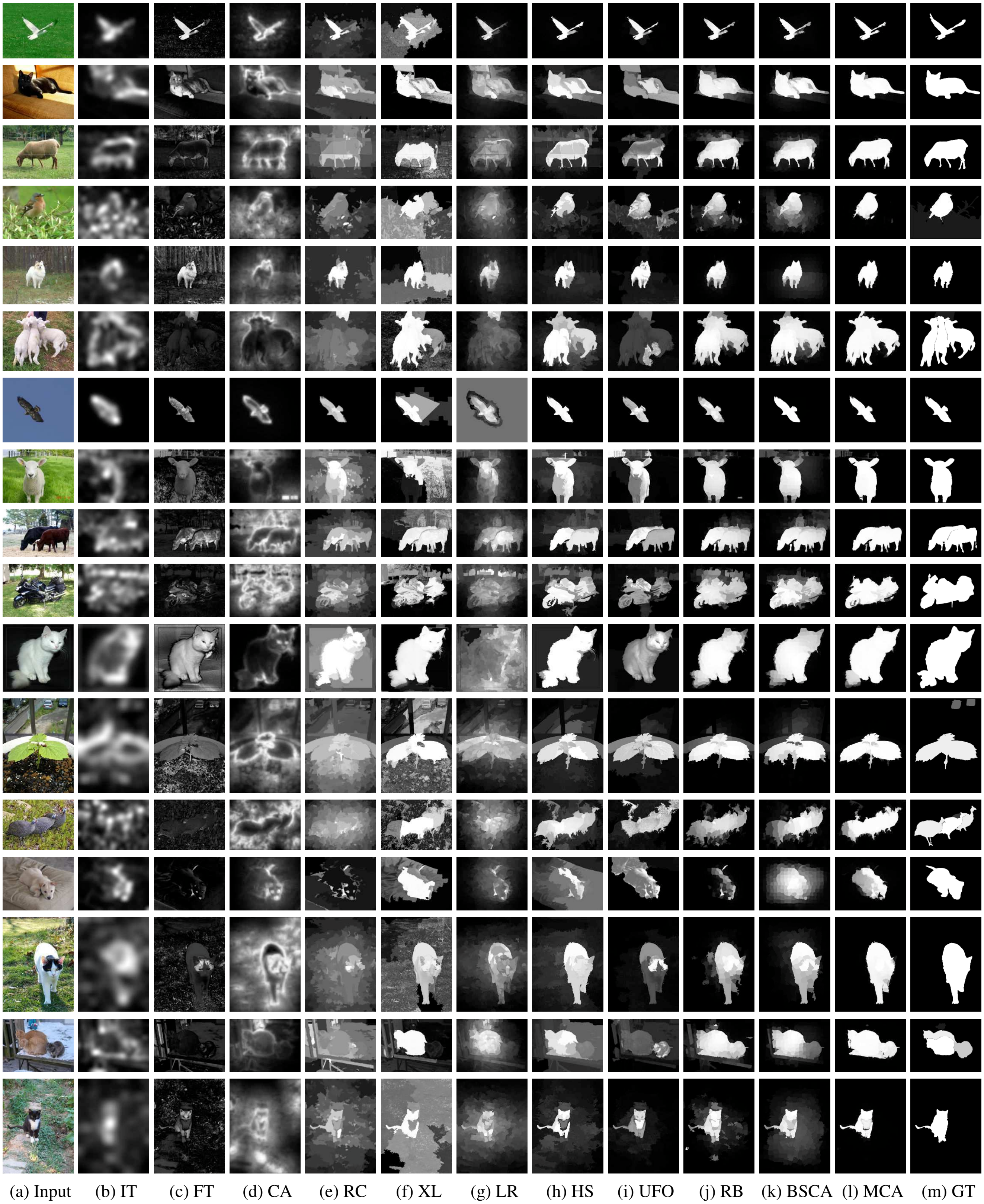

Figure 5. Comparison of different saliency maps on PASCAL-S. BSCA: The background-based maps optimized by Single-layer Cellular Automata. MCA: The integrated saliency maps via Multi-layer Cellular Automata. GT: Ground Truth.

We compare more saliency maps generated by different methods and their optimized versions with Single-layer Cellular Automata (SCA). These methods include IT98 [5], FT09 [1], CA10 [4], RC11 [3], XL13 [10], LR12 [9], HS13 [11], UFO13 [6], RB14 [12]. We display the results tested on five public datasets: ASD [1], MSRA-5000 [8], THUS [2], ECSSD [11] and PASCAL-S [7].

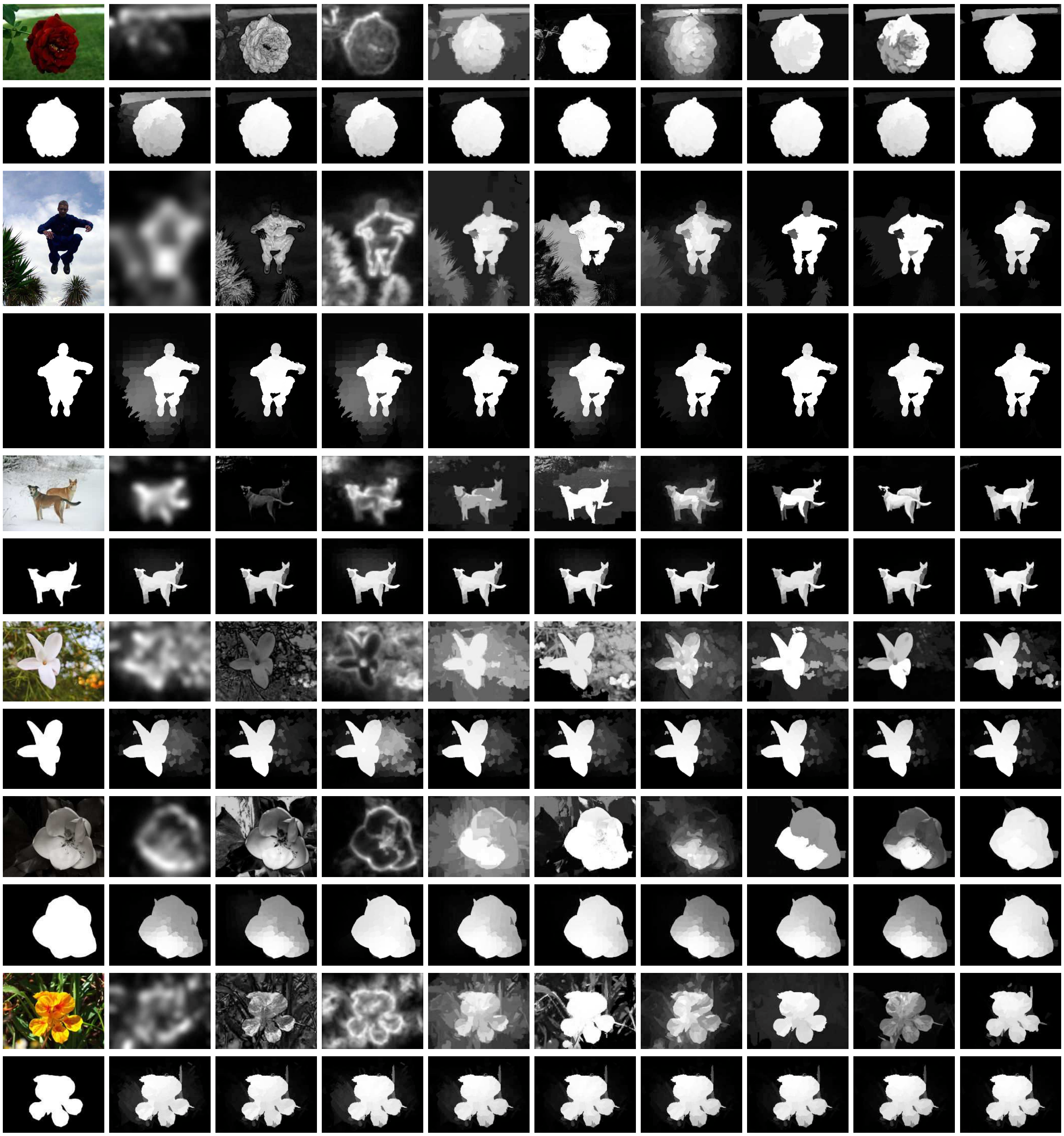

(a) Input (b) IT (c) FT (d) CA (e) RC (f) XL (g) LR (h) HS (i) UFO (j) RB

Figure 6. Comparison of different saliency maps generated by nine state-of-the-art methods and optimized by Single-layer Cellular Automata on ASD. The saliency maps in the odd rows are original results. The saliency maps displayed in the even rows are the optimized results. Input images and ground truth are presented in the first column.

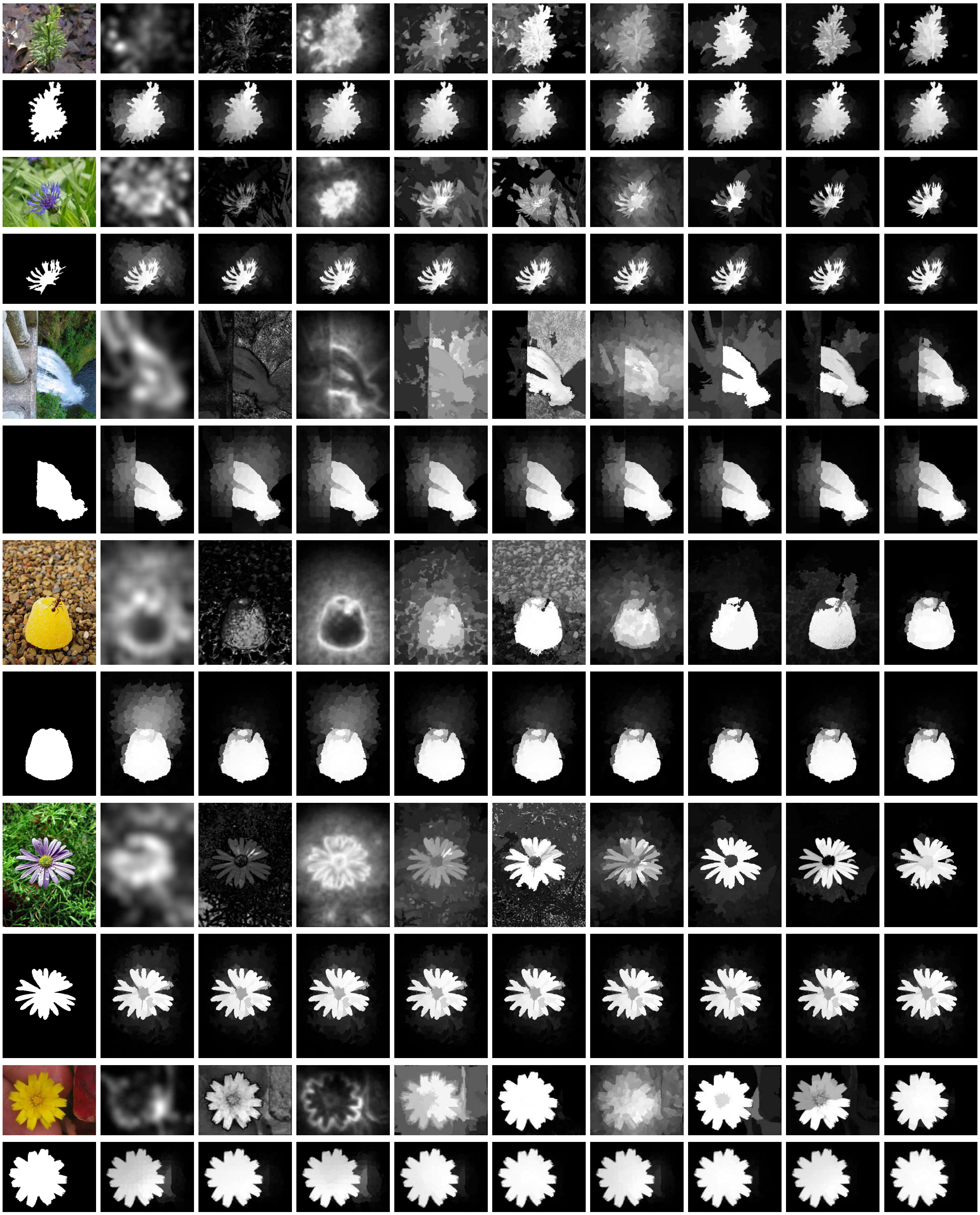

(a) Input (b) IT (c) FT (d) CA (e) RC (f) XL (g) LR (h) HS (i) UFO (j) RB

Figure 7. Comparison of different saliency maps generated by nine state-of-the-art methods and optimized by Single-layer Cellular Automata on MSRA-5000. The saliency maps in the odd rows are original results. The saliency maps displayed in the even rows are the optimized results. Input images and ground truth are presented in the first column.

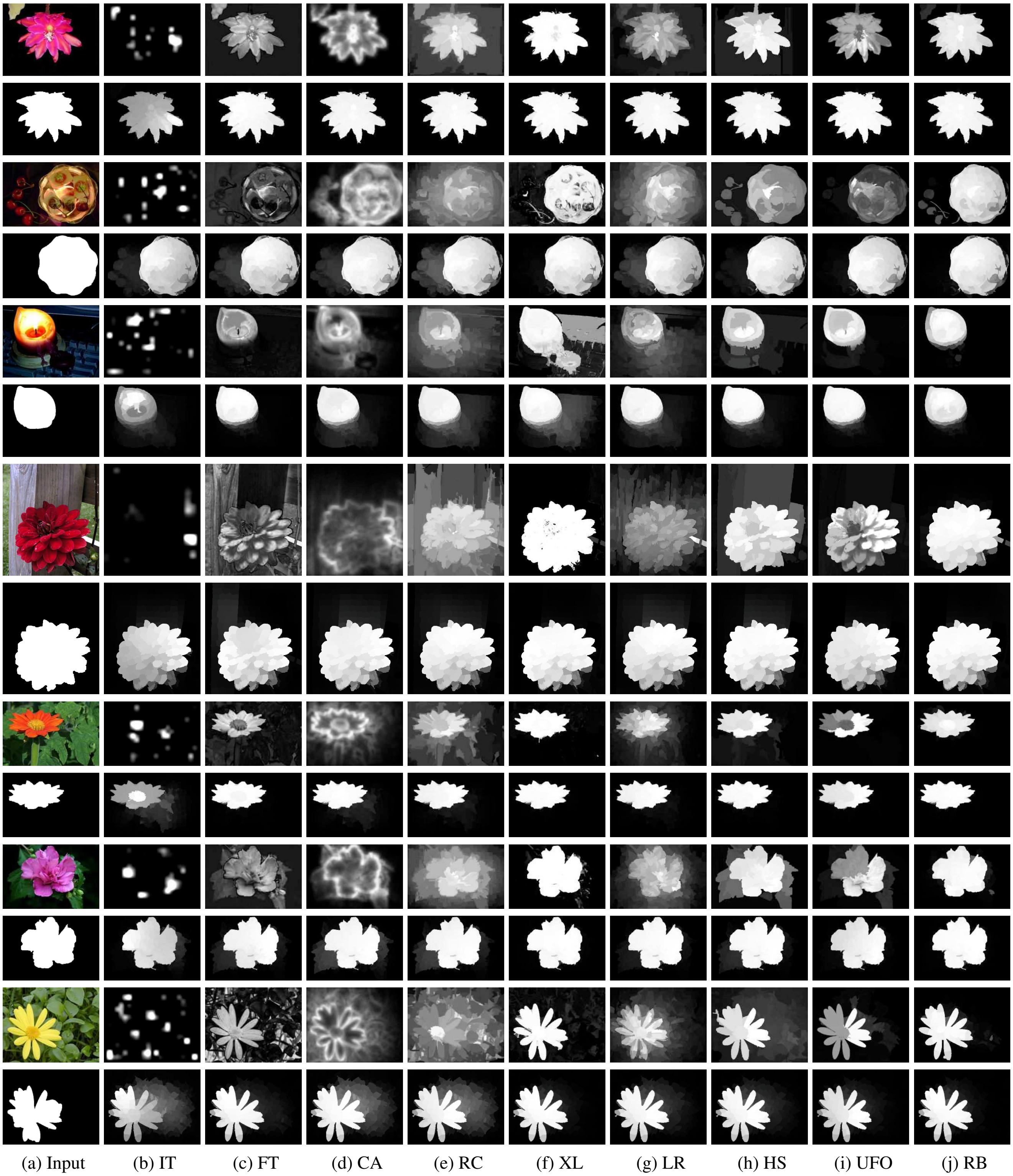

Figure 8. Comparison of different saliency maps generated by nine state-of-the-art methods and optimized by Single-layer Cellular Automata on THUS-10000. The saliency maps in the odd rows are original results. The saliency maps displayed in the even rows are the optimized results. Input images and ground truth are presented in the first column.

(a) Input (b) IT (c) FT (d) CA (e) RC (f) XL (g) LR (h) HS (i) UFO (j) RB

Figure 9. Comparison of different saliency maps generated by nine state-of-the-art methods and optimized by Single-layer Cellular Automata on ECSSD. The saliency maps in the odd rows are original results. The saliency maps displayed in the even rows are the optimized results. Input images and ground truth are presented in the first column.

Figure 10. Comparison of different saliency maps generated by nine state-of-the-art methods and optimized by Single-layer Cellular Automata on PASCAL-S. The saliency maps in the odd rows are original results. The saliency maps displayed in the even rows are the optimized results. Input images and ground truth are presented in the first column.

References

[1] R. Achanta, S. Hemami, F. Estrada, and S. Susstrunk. Frequency-tuned salient region detection. In *Computer Vision and Pattern Recognition, 2009. CVPR 2009. IEEE Conference on*, pages 1597–1604. IEEE, 2009.

[2] M.-M. Cheng, N. J. Mitra, X. Huang, P. H. Torr, and S.-M. Hu. Salient object detection and segmentation. *Image*, 2(3):9, 2011.

[3] M.-M. Cheng, G.-X. Zhang, N. J. Mitra, X. Huang, and S.-M. Hu. Global contrast based salient region detection. In *Computer Vision and Pattern Recognition (CVPR), 2011 IEEE Conference on*, pages 409–416. IEEE, 2011.

[4] S. Goferman and A. L Tal. context-aware saliency detection. *Computer*, 2010.

[5] L. Itti, C. Koch, and E. Niebur. A model of saliency-based visual attention for rapid scene analysis. *IEEE Transactions on pattern analysis and machine intelligence*, 20(11):1254–1259, 1998.

[6] P. Jiang, H. Ling, J. Yu, and J. Peng. Salient region detection by ufo: Uniqueness, focusness and objectness. In *Computer Vision (ICCV), 2013 IEEE International Conference on*, pages 1976–1983. IEEE, 2013.

[7] Y. Li, X. Hou, C. Koch, J. Rehg, and A. Yuille. The secrets of salient object segmentation. CVPR, 2014.

[8] T. Liu, Z. Yuan, J. Sun, J. Wang, N. Zheng, X. Tang, and H.-Y. Shum. Learning to detect a salient object. *Pattern Analysis and Machine Intelligence, IEEE Transactions on*, 33(2):353–367, 2011.

[9] X. Shen and Y. Wu. A unified approach to salient object detection via low rank matrix recovery. In *Computer Vision and Pattern Recognition (CVPR), 2012 IEEE Conference on*, pages 853–860. IEEE, 2012.

[10] Y. Xie, H. Lu, and M.-H. Yang. Bayesian saliency via low and mid level cues. *Image Processing, IEEE Transactions on*, 22(5):1689–1698, 2013.

[11] Q. Yan, L. Xu, J. Shi, and J. Jia. Hierarchical saliency detection. In *Computer Vision and Pattern Recognition (CVPR), 2013 IEEE Conference on*, pages 1155–1162. IEEE, 2013.

[12] W. Zhu, S. Liang, Y. Wei, and J. Sun. Saliency optimization from robust background detection. In *Computer Vision and Pattern Recognition (CVPR), 2014 IEEE Conference on*, pages 2814–2821. IEEE, 2014.